Z^{0}-boson production in association with a tt[over ¯] pair at next-to-leading order accuracy with parton shower effects

M. V. Garzelli, A. Kardos, C. G. Papadopoulos, and Z. Trócsányi

Z^0-boson production in association with a top anti-top pair at NLO accuracy with parton shower effects

M. V. Garzelli,[1,2] A. Kardos,[1,3] C. G. Papadopoulos,[4] and Z. Trócsányi[1,3]

[1]*Institute of Physics, University of Debrecen,*

H-4010 Debrecen P.O.Box 105, Hungary

[2]*Laboratory for Astroparticle Physics,*

University of Nova Gorica, SI-5000 Nova Gorica, Slovenia

[3]*Institute of Nuclear Research of the Hungarian Academy of Sciences, Hungary*

[4]*Institute of Nuclear Physics, NCSR Demokritos, GR-15310 Athens, Greece*

Abstract

We present predictions for the production cross section of a Standard Model Z^0-boson in association with a $t\bar{t}$ pair at the next-to-leading order accuracy in QCD, matched with shower Monte Carlo programs to evolve the system down to the hadronization energy scale. We adopt a framework based on three well established numerical codes, namely the `POWHEG-BOX`, used for computing the cross section, `HELAC-NLO`, which generates all necessary input matrix elements, and finally a parton shower program, such as `PYTHIA` or `HERWIG`, which allows for including t-quark and Z^0-boson decays at the leading order accuracy and generates shower emissions, hadronization and hadron decays.

PACS numbers: 12.38.Bx, 13.87.-a, 14.65.Ha, 14.70.Hp

I. INTRODUCTION

With increasing collider energies, the t-quark plays an increasingly important role in particle physics. Its production cross section grows faster with energy than that of any other discovered Standard Model (SM) particle. Already after the first year of successful run of the LHC, the $t\bar{t}$ production cross section is measured with unprecedented accuracy at $\sqrt{s} = 7\,\mathrm{TeV}$, so that the corresponding SM theoretical prediction will be challenged soon [1, 2]. For instance, the CMS collaboration measured $\sigma_{t\bar{t}} = 154 \pm 18\,\mathrm{pb}$ as compared to the theoretical predictions $\sigma_{t\bar{t}}^{\mathrm{NNLOapprox}} = 164^{+10}_{-14}\,\mathrm{pb}$ [3], or $\sigma_{t\bar{t}}^{\mathrm{NNLOapprox}} = 163^{+11}_{-10}\,\mathrm{pb}$ [4]. However, many other t-quark properties have not yet been directly accessed. In particular, its couplings to neutral gauge (especially the Z^0) and scalar bosons are still prone to large uncertainties. In Refs. [5, 6] the possibility of measuring the $t\bar{t}Z$ and $t\bar{t}\gamma$ couplings was studied based upon leading-order (LO) parton level predictions. Although such precision is sufficient for feasibility studies, finding the optimal values of the experimental cuts requires indeed predictions at higher accuracy.

An essential step towards higher accuracy is the inclusion of next-to-leading order (NLO) radiative corrections. Recent theoretical advances made possible our computation of the $pp \to t\bar{t}Z$ cross section at the parton level, including QCD corrections at NLO [7]. In order though to get the optimum benefit and to produce predictions that can be directly compared to experimental data at the hadron level, a matching with parton shower (PS) and hadronization implemented in shower Monte Carlo (SMC) programs is ultimately inevitable. Thus, in this letter we present first predictions for $pp \to t\bar{t}Z$ production at LHC at the matched NLO + PS accuracy.

II. METHOD

In constructing a general interface of PS to matrix element (ME) computations with NLO accuracy in QCD, we have chosen to combine the POWHEG [8, 9] method and FKS subtraction scheme [10], as implemented in the `POWHEG-BOX` [11] computer framework, with the HELAC-NLO [12] approach. In particular, `POWHEG-BOX` requires the relevant ME's as external input. We obtain the latter in a semi-automatic way by codes in the `HELAC-NLO` package [13]. With this input `POWHEG-BOX` is used to generate events at the Born plus
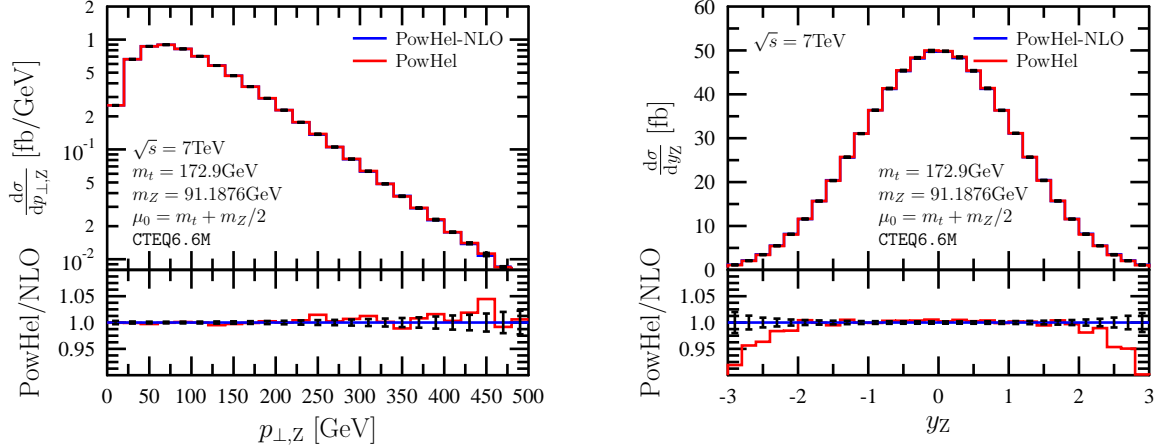
Figure 1. Inclusive transverse momentum (left) and rapidity (right) distributions of the Z^0-boson at exact NLO level (blue solid line, PowHel-NLO, see Ref. [7]) and after first radiation (red solid line, PowHel level) at the present LHC energy. The lower panels show the ratio of the two predictions (PowHel/PowHel-NLO) with combined statistical uncertainties.

first radiation emission level, stored in Les Houches Event Files (LHEF) [14], that can be interfaced to standard SMC programs. Previous applications of the whole framework, proving its robustness, were presented in Refs. [15, 16]. This same setup also allows for exact NLO pure hard-scattering predictions. Further details on the implementation of the computation of the pp $\rightarrow$ t$\bar{\text{t}}Z$ hard-scattering cross-section in it, at NLO accuracy in QCD, together with checks, were recorded in Ref. [7].

All these computations are steps of an ongoing project for generating event samples for $pp \rightarrow$ t$\bar{\text{t}}X$ processes, where X stays for a hard partonic object [17]. The events we generate are stored in LHEF, made available on the web [18], and are ready to be interfaced to standard SMC programs to produce predictions for distributions at the hadron level. Such predictions can be useful for optimizing the selection cuts applied to disentangle the signal from the background, in order to improve the experimental accuracy of the t-quark coupling measurements.

Interfacing NLO calculations to SMC programs allows to estimate the effects of decays, shower emissions and hadronization, therefore we have analyzed the process at hand at three different stages of evolution:

PowHel: we analyzed the events including no more parton emissions than the first and hardest one, collected in LHEF produced as output of `POWHEG-BOX` + `HELAC-NLO`

(PowHel).

Decay: we just included on-shell decays of t-quarks and the Z^0-boson, as implemented in PYTHIA [19], and further decays of their decay products, like charged leptons (the τ is considered as unstable) and gauge bosons (W), turning off any other initial- and final-state PS and hadronization effect.

Full SMC: particle decays, shower evolution, hadronization and hadron decays have been included in our simulations, using both PYTHIA and HERWIG [20].

In our computation, we adopted the following parameters: $\sqrt{s} = 7\,\mathrm{TeV}$ or $\sqrt{s} = 14\,\mathrm{TeV}$, CTEQ6.6M PDF set from LHAPDF, with a 2-loop running α_s, 5 light flavours and $\Lambda_5^{\overline{\mathrm{MS}}} = 226\,\mathrm{MeV}$, $m_t = 172.9\,\mathrm{GeV}$, $m_Z = 91.1876\,\mathrm{GeV}$, $G_F = 1.16639 \cdot 10^{-5}\,\mathrm{GeV}^{-2}$. The renormalization and factorization scales were chosen equal to the default scale $\mu_0 = m_t + m_Z/2$. We used the last version of the SMC fortran codes: PYTHIA 6.425 and HERWIG 6.520. Following our implementation of $t\bar{t}H$ hadroproduction in Ref. [16], in both SMC setup muons (default in PYTHIA) and neutral pions were assumed as stable particles. All other particles and hadrons were allowed to be stable or to decay according to the default implementation of each SMC. Masses and total decay widths of the elementary particles were tuned to the same values in PYTHIA and HERWIG, but each of the two codes was allowed to compute autonomously partial branching fractions in different decay channels for all unstable particles and hadrons. Multiparticle interaction effects were neglected (default in HERWIG). Additionally, the intrinsic $p_\perp$-spreading of valence partons in incoming hadrons in HERWIG was assumed to be 2.5 GeV.

III.   CHECKS

To check event generation, we compared several distributions from events including no more than first radiation emission (PowHel level) with the exact NLO predictions of Ref. [7]. We found agreement for all considered observables within a very few percent (typically $1 - 2\%$), except in the tails of the distributions, where the agreement can decrease, due to limited statistics and/or to the larger sensitivity to the matching of the fixed order computation to the PS. As examples, we show in Fig. 1 the transverse momentum and rapidity distributions of the Z^0-boson, drawn by considering a sample of about 3 million

unweighted events at LHC at $\sqrt{s} = 7$ TeV center-of-mass energy. As for the rapidity of the Z^0-boson, the agreement between exact NLO predictions and predictions including no more than first radiation emission is well below 1% in the central region, and decreases staying within $5-10\%$ for Z^0 emitted in the forward (or backward) direction, whereas, as for the transverse momentum, the agreement is well within $1-2\%$ for $p_\perp^Z < 350$ GeV and decreases within 5% for higher $p_\perp^Z$, as can be understood from the lower insets of each panel, where we plot the ratio of the two values (LHEF/exact NLO). As for the $p_\perp^Z$ distribution plot, we can explain the small disagreement in the high $p_\perp^Z$ tail just in terms of low statistics in the corresponding bins, as can be understood by observing that the ratio of the two values oscillates around one, whereas, in the rapidity distribution plot, a modest PS effect, due to first radiation emission, leading to a change in the momenta of the other particles in the same direction, gives a systematic decrease of the results for the rapidity of the Z^0 at the LHEF level, with respect to the results at the exact NLO level, in the rapidity tails. We can conclude that for $t\bar{t}Z$ the level of agreement between the inclusive distributions at the NLO and LHEF level is similar to the one we already reported in previous papers, in the study of the $t\bar{t}$+jet and $t\bar{t}H$ processes, and that our $t\bar{t}Z$ results suggest we have a good control of the matching phase, thus we can proceed further.

Next, we studied the effect of the full SMC by comparing distributions at the decay and SMC level. Since particle yields are very different at the end of these two stages, we first made such a comparison without any selection cut, in order to avoid the introduction of any bias. As an illustrative example, we present in Fig. 2 the distributions of the transverse momentum and rapidity of the hardest jet, $p_\perp^j$ and y_j, again at the $\sqrt{s} = 7$ TeV LHC. Jets are reconstructed through the anti$-k_\perp$ algorithm with $R = 0.4$, as implemented in `FastJet` [21]. The softening of the transverse momentum spectrum is apparent as going from the decay level to the full SMC one, amounting to about a 20% decrease in the high $p_\perp^j$ tail, and increase up to a factor of ~ 2 - 10 the content of the lower $p_\perp^j$ bins, which amounts to an almost uniform shift of the distributions to lower values by about the width of one bin. On the other hand, the effect of the shower on the rapidity of the hardest jet is almost negligible and rather homogeneous, even if slightly sensitive to the details of the PS description, as better explained below. The cross-section at both level amounts to $\sigma = 138.70 \pm 0.01$ fb (the uncertainties quoted here and in the following can be ascribed to limited statistics of the event sample, only). Using our setup for the full SMC's, we found agreement between
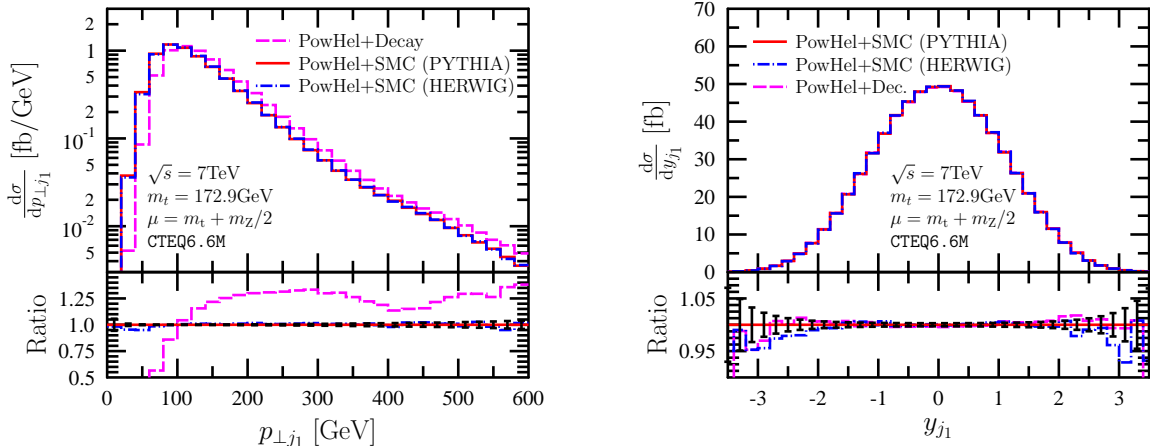
Figure 2. Inclusive transverse momentum (left) and rapidity (right) distributions of the hardest jet after decay (simulated by means of PYTHIA, pink dashed line) and after full SMC, by considering both PYTHIA (red solid line) and HERWIG (blue dash-dotted line). The lower panels show the ratio of all predictions to PowHel+SMC using PYTHIA.

PYTHIA and HERWIG predictions within very few percent, despite the conceptual differences between the two SMC generators as for the shower ordering variables and hadronization models, confirming the level of agreement already reported in Ref. [16] in the study of a different process ($t\bar{t}H$). The largest differences between the effects of the two SMC's can be observed in the rapidity spectra: as shown in Fig. 2, HERWIG emissions are slightly more central than the PYTHIA ones, giving rise to slightly steeper spectra, a behaviour already found both in Ref. [22] and in Ref. [16] in the study of different processes.

IV. PREDICTIONS

We turn to making predictions for $t\bar{t}Z$ hadroproduction at the LHC including experimental selection cuts. For this analysis, in the absence of a dedicated tune for NLO matched computations, PYTHIA was tuned to the Perugia 2011 set of values, one of the most recent LO tunes [23], updated on the basis of recent LHC data, providing a $p_\perp$-ordered PS. Its application turned out to increase our particle yields by about 10 %. As a consequence, the agreement between the tuned PYTHIA and untuned HERWIG predictions decreases (as for HERWIG, the default configuration was used, providing instead an angular-ordered PS), and we present only the PYTHIA ones.

In case of $t\bar{t}Z$ hadroproduction overwhelming backgrounds come from $t\bar{t}$+jets final states. In Ref. [6] the differential cross section as a function of missing transverse momentum for the production of $\not{p}_\perp b\bar{b}$+4 jets was found a useful tool for differentiating the signal and the possible backgrounds. The proposed full set of selection cuts is rather exclusive and mainly aims at selecting the $Z^0 \to \nu\bar{\nu}$ decay channel, in combination with the fully hadronic decay channels of the t- and $\bar{t}$-quarks. The proposed set of cuts is certainly effective when applied to a leading order hard-scattering scenario at $\sqrt{s} = 14\,\text{TeV}$ energy, without the complications arising from the existence of further higher-order emissions. In this paper, we try to extend it to this more complicated case, and to lower energies. We thus applied the full extended set of cuts described below in the analysis of samples of 3 million simulated events at both $\sqrt{s} = 7\,\text{TeV}$ and $\sqrt{s} = 14\,\text{TeV}$ center-of-mass energies, and we observed that the rates decrease so much that the measurement for the present LHC run at $\sqrt{s} = 7\,\text{TeV}$ looks quite demanding from the statistical point of view ($\sigma_{\text{all cut},14}/\sigma_{\text{all cut},7} \sim 7$ and 8 at the decay and at the full SMC level, respectively), therefore, we restrict our study to present predictions for the future runs at $\sqrt{s} = 14\,\text{TeV}$.

In order to assess the effect of different cuts, and to understand which are the most effective ones in disentangling the signal from the background, we considered two set of cuts: a reduced set, including most but not all cuts, and the full one, as outlined in the following.

First we consider the following reduced set of cuts: 1) we reconstruct at least six jets with rapidity $|y| < 2.5$, 2) of these we require at least one b-jet and one $\bar{b}$-jet, 3) for b-jets $p_\perp^b > 20\,\text{GeV}$, 4) for other jets $p_\perp^{\text{non}-b} > 30\,\text{GeV}$, 5) at least 3 jets ($b$ or non-b) with $p_\perp^j > 50\,\text{GeV}$, 6) $\Delta R(j,j) > 0.4$, where j denotes any (b or non-b) jet and ΔR is defined as $\sqrt{\Delta\phi^2 + \Delta y^2}$, 7 − 8) $\Delta\phi(\not{p}_\perp, p_{\perp,j}) > 100°$, with $p_{\perp,j}$ meaning either $(p_\perp(\hat{b}_1) + p_\perp(\hat{\bar{b}}_2))$ (cut 7), or $(p_\perp(\hat{j}_1) + p_\perp(\hat{j}_2) + p_\perp(\hat{j}_3) + p_\perp(\hat{j}_4))$ (cut 8), where $\hat{b}_1, \hat{\bar{b}}_2$ and $\hat{j}_1, \hat{j}_2, \hat{j}_3, \hat{j}_4$ are the jets that allow for the best $\text{t} \to \text{b}W^+ \to bjj$ and $\bar{\text{t}} \to \bar{\text{b}}W^- \to \bar{b}jj$ invariant mass simultaneous reconstruction, by minimizing the

$$\chi^2(b_1 j_1 j_2; \bar{b}_2 j_3 j_4) = \frac{(m_{j_1 j_2} - m_W)^2}{\sigma_W^2} + \frac{(m_{j_3 j_4} - m_W)^2}{\sigma_W^2}$$
$$+ \frac{(m_{b_1 j_1 j_2} - m_W)^2}{\sigma_{\text{t}}^2} + \frac{(m_{\bar{b}_2 j_3 j_4} - m_W)^2}{\sigma_{\text{t}}^2},$$

computed by considering all possible $j_k j_l$, $b_i j_k j_l$ and $\bar{b}_i j_k j_l$ combinations. The $W \to jj$ and $\text{t} \to bjj$ invariant mass resolutions were set to $\sigma_W = 7.8\,\text{GeV}$ and $\sigma_t = 13.4\,\text{GeV}$, respectively
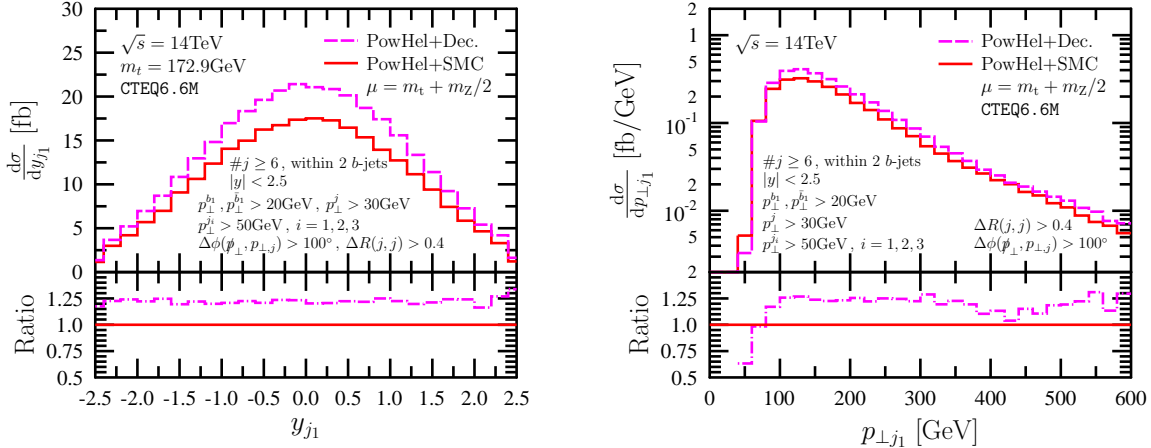
Figure 3. Rapidity (left) and transverse momentum (right) distributions of the hardest jet after decay and after full SMC (PYTHIA), under selection cuts (1–8) implemented at both levels. The lower panels show the ratio of the predictions at different levels (decay/SMC).

[24].

In Fig. 3 we show the distributions of the rapidity and transverse momentum of the hardest jet under the reduced set of cuts. From the left panel it is evident that the effect of the cuts on the rapidity distribution of the hardest jet is uniform, when the cuts are applied after full SMC, with respect to the case they are instead applied at the decay level, decreasing of almost an equal amount ($\sim 20\%$) the population of each rapidity bin. On the other hand, the transverse momentum spectrum of the hardest jet, selected by the cuts and shown in the right panel, becomes softer when going from the decay to the full SMC level, a behaviour similar to the one already observed in the absence of cuts (see Fig. 2 for comparison), the main difference being the area spanned by the distributions, i.e. their integral. The PowHel+PYTHIA cross sections after these cuts amount to $\sigma_{\text{dec}} = 65.56 \pm 0.15 \, \text{fb}$ and $\sigma_{\text{SMC}} = 53.74 \pm 0.13 \, \text{fb}$, at the decay and at the SMC level, respectively.

In Fig. 4 we plot the invariant mass distribution of the t-quark, as reconstructed from its decay products, by minimizing the χ^2 above, under the same reduced set of cuts. At the decay level, the reconstruction leads to a clear peak centered around the m_t value (blue dash-dotted line extending over the whole abscissa interval). On the other hand, after full SMC, due both to further emissions which modify jet content and to hadron decays, there are more candidate jets and the reconstruction is less successful (red solid line extending over the whole abscissa interval). Although a peak is still visible (more evident in non-log
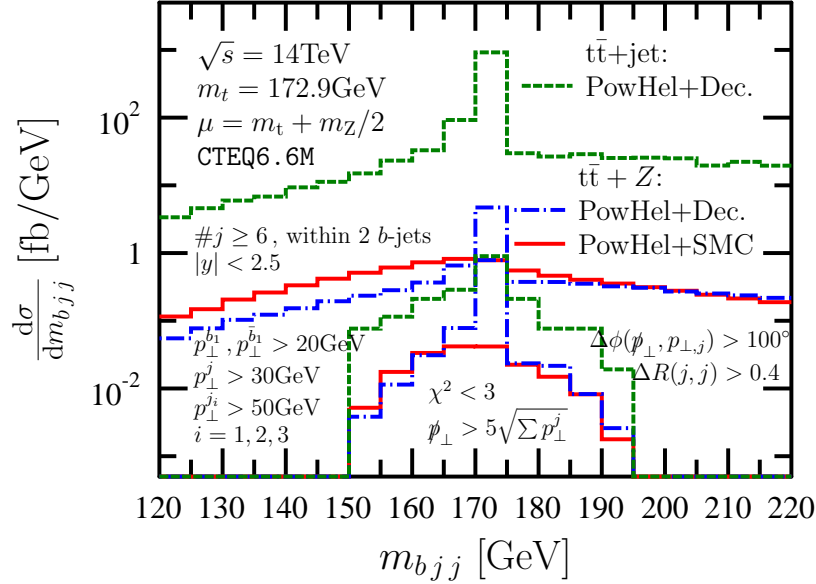
8

Figure 4. Invariant mass distribution of the t-quark reconstructed from the decay products at both decay (blue dash-dotted lines) and full SMC (red solid lines) levels, for the $t\bar{t}Z$ signal and, at the decay level, for one background ($t\bar{t}$+jet) (green dashed lines) after selection cuts (1–8) (wider distributions in abscissa values) and after selection cuts (1–10) (narrower distributions).

scale), it is smeared towards lower mass values. The effect of the shower and hadronization turns out to be especially large in the peak region, largely smearing the peak, and populating the bins corresponding to lower invariant mass values, corresponding to lighter jets, due to PS emissions, or to the fragmentation of heavy jets, taking into account the possibility that heavy hadrons may decay in lighter ones by emitting leptons and neutrinos.

In Fig. 4 we also show the m_{bjj} distribution after decay for an important background process: $t\bar{t}$-pair production associated with a jet (obtained at the scale $\mu_0 = m_t$), under the same cuts (green dashed line extending over the whole abscissa range). Clearly, the background overwhelms the signal by more than two orders of magnitude in the peak region, therefore, in order to select the peak region and to reduce the background, we include two more cuts: 9) missing transverse momentum $\not{p}_\perp$ (due to all ν's) $> 5\,\mathrm{GeV}^{1/2}\sqrt{\sum_j p_\perp^j}$ (of all jets, b or non-b), and 10) $\chi^2_{\min} < 3$, where $\chi^2_{\min}$ is the minimum of the χ^2 above. Thus, we closely reproduce the cuts in Ref. [6], aimed at favoring the $Z^0 \to \nu\nu$ decay channel. However, one has should take into account that, at the full SMC level, a non-negligible contribution to

$p_\perp$ come from the decay of the B-hadrons. In collider experiments, neutrinos are not detected individually, but $p_\perp$ is obtained as a whole (vectorial sum) from the measured momenta of the observed particles. This means that in practice it is very difficult to disentangle the missing energy component coming from the decay of the Z^0 vector boson, from the one coming instead from the decay of the B-hadrons. This complication, present in the full SMC scenario, is not present in the simplified one offered by the decay case, where hadronization is not included, implying that a cut like cut 9) is more effective at the decay level than at the SMC one. As for cut 10), it is intended to just select the events where top and antitop reconstruction is more successful. Even this cut is more easily fulfilled at the decay than at the SMC level, due to the incresed number of lighter jets and possible jet combinations, as already explained above. The effect of the whole set of cuts on top reconstruction in $t\bar{t}Z$ and $t\bar{t}$+jet events is also shown in Fig. 4 (lines extending over the $150 < m_{bjj} < 195$ GeV interval). Although this set of cuts is effective in selecting the signal, the background is globally still larger: for the signal $\sigma_{\mathrm{dec}} = 4.83 \pm 0.04$ fb, while for the background $\sigma_{\mathrm{dec}} = 9.86 \pm 1.05$ fb, at the decay level. However, as can be understood from Fig. 5, where the distributions of the missing transverse momentum after decay are shown for both $t\bar{t}Z$ and $t\bar{t}$+jet, these cuts allow for disentangling the signal, at least at the decay level. At the shower level, the $p_\perp$ distributions of the $t\bar{t}Z$ signal still shows a harder spectrum than the one of the $t\bar{t}$+jet background, but to a lesser extent. In this case, the effect of different top reconstruction strategies, still under investigation, can be crucial to help better disentangle the signal from the background in the $p_\perp b\bar{b}$+4 jets considered channel. A further issue affecting top reconstruction, requiring further work beyond the scope of this paper, is represented by the fact that the present experimental values of b-jet tagging efficiencies, reached at the LHC experiments, are still far from the 100% assumed in this paper.

V. CONCLUSIONS

We studied the hadroproduction of a Z^0 boson in association with a $t\bar{t}$-pair, process of interest for measuring the $t\bar{t}Z$-coupling directly at the LHC. We studied the effect of heavy particle decays as well as the one of the full SMC. We produced predictions for the LHC. As the production cross section is rather small, measuring the $t\bar{t}Z$-coupling becomes more feasible after the planned 14 TeV energy upgrade. We also consider the effects of the $t\bar{t}$+jet
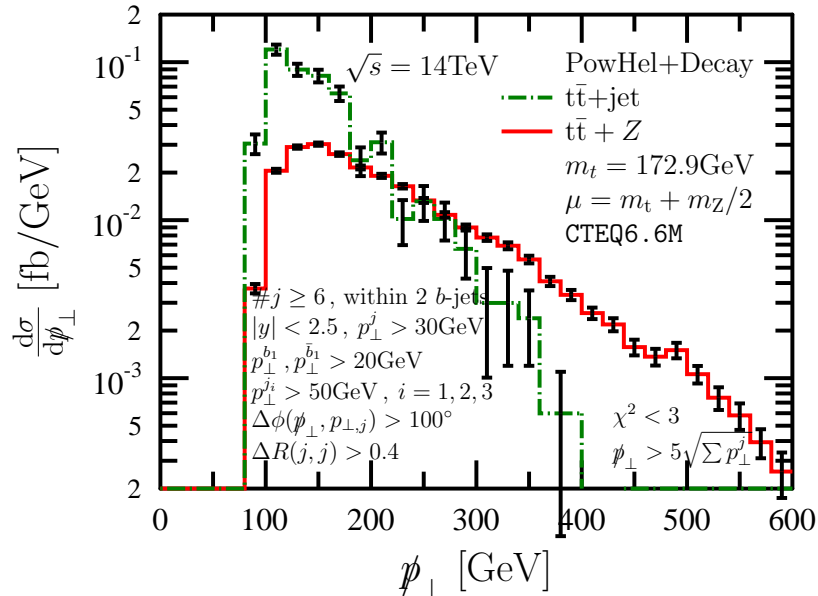
Figure 5. Distribution of the missing transverse momentum after decay, under physical cuts (1–10) applied to the signal ($t\bar{t}Z$, solid line) and to one background ($t\bar{t}$+jet, dash-dotted line).

background with respect to the $t\bar{t}Z$ signal, by studying the $t\bar{t}$+jet process under the same system of cuts. Once all background processes will be predicted with the same accuracy, our predictions will make possible a realistic optimization of the experimental cuts.

Our studies show that the efficiency of the selection cuts devised at the parton level in a LO study may be seriously affected by the higher order (NLO+PS) plus hadronization effects. Thus it is important to explore other, more efficient selections of the $t\bar{t}Z$ events, especially with respect to the reconstruction of the t-quarks from either simulation results or experimental data after hadron decay. Our LHEF events make possible such explorations, which we plan in a forthcoming work.

ACKNOWLEDGMENTS

---

[1] M. Saleem, arXiv:1109.3912.

[2] S. Chatrchyan *et al.* [CMS Collaboration], Phys. Rev. D **84**, 092004 (2011) [arXiv:1108.3773].

[3] M. Aliev, H. Lacker, U. Langenfeld, S. Moch, P. Uwer and M. Wiedermann, Comput. Phys. Commun. **182**, 1034 (2011) [arXiv:1007.1327].

[4] N. Kidonakis, Phys. Rev. D **82**, 114030 (2010) [arXiv:1009.4935].

[5] U. Baur, A. Juste, L. H. Orr and D. Rainwater, Phys. Rev. D **71**, 054013 (2005) [arXiv:hep-ph/0412021].

[6] U. Baur, A. Juste, L. H. Orr and D. Rainwater, Phys. Rev. D **73**, 034016 (2006) [arXiv:hep-ph/0512262].

[7] A. Kardos, C.G. Papadopoulos and Z. Trócsányi, arXiv:1111.0610.

[8] P. Nason, JHEP **0411**, 040 (2004) [arXiv:hep-ph/0409146].

[9] S. Frixione, P. Nason and C. Oleari, JHEP **0711**, 070 (2007) [arXiv:0709.2092].

[10] S. Frixione, Z. Kunszt, A. Signer, Nucl. Phys. B **467**, 399 (1996) [arXiv:hep-ph/9512328].

[11] S. Alioli, P. Nason, C. Oleari and E. Re, JHEP **1006**, 043 (2010) [arXiv:1002.2581].

[12] G. Bevilacqua *et al.*, Nucl. Phys. Proc. Suppl. **205-206**, 211 (2010) [arXiv:1007.4918].

[13] G. Bevilacqua *et al.*, arXiv:1110.1499.

[14] J. Alwall *et al.*, Comput. Phys. Commun. **176**, 300 (2007) [arXiv:hep-ph/0609017].

[15] A. Kardos, C. Papadopoulos and Z. Trócsányi, Phys. Lett. B **705**, 76 (2011) [arXiv:1101.2672].

[16] M. V. Garzelli, A. Kardos, C. G. Papadopoulos and Z. Trócsányi, Europhys. Lett. **96**, 11001 (2011) [arXiv:1108.0387].

[17] M.V. Garzelli, A. Kardos and Z. Trócsányi, arXiv:1111.1446.

[18] http://grid.kfki.hu/twiki/bin/view/DbTheory/.

[19] T. Sjostrand, S. Mrenna and P. Z. Skands, JHEP **0605**, 026 (2006) [arXiv:hep-ph/0603175].

[20] G. Corcella *et al.*, arXiv:hep-ph/0210213.

[21] M. Cacciari, G. P. Salam and G. Soyez, JHEP **04**, 063 (2008) [arXiv:0802.1189].

[22] C. Oleari and L. Reina, JHEP **08**, 061 (2011); Erratum-ibid. **11**, 040 (2011) [arXiv:1105.4488].

[23] P. Z. Skands, Phys. Rev. D **82**, 074018 (2010) [arXiv:1005.3457].

[24] M. Beneke *et al.*, arXiv:hep-ph/0003033, in the Report of the "1999 CERN Workshop on SM physics (and more) at the LHC", 419-529.